

# MILI: Biophotonics Technology for In-Situ, Fast, Accurate and Cost-Effective Milk Analysis

Panayiota Demosthenous<sup>1</sup> <sup>a</sup>, Maria Aspri<sup>2</sup> <sup>b</sup>, Maria Moyseos<sup>1</sup> <sup>c</sup> and Marios Sergides<sup>1</sup> <sup>d</sup>

<sup>1</sup>Cy.R.I.C. Cyprus Research and Innovation Center Ltd, 28th October Avenue, 2414 Nicosia, Cyprus

<sup>2</sup>Dept. of Agricultural Sciences, Biotechnology and Food Science, Cyprus University of Technology, 3036 Limassol, Cyprus  
{p.demosthenous, maria.moyseos, m.sergides}@cyric.eu, maria.aspri@cut.ac.cy

**Keywords:** Fluorometry, Biophotonics, Biosensors, Optical Analysis, Automated System, Food Safety, Milk Analysis, Embedded Electronics.


**Abstract:** Contaminated milk poses serious health risks to consumers, highlighting the need for efficient detection methods. Currently, the dairy industry relies on precise but time-consuming laboratory methods that require specialized personnel. The work presented here aims to address this by developing a fast, cost-effective and reliable system for detecting common contaminants in milk at the farm level. The MILI device is based on state-of-the-art biophotonics, combining customised biosensors, optical analysis, electronics, and software modules. The detection method relies on the use of fluorometry, where the signal originating from labelled antibodies bound to specific analytes (antibiotics and toxins) is measured. Two different chromophore molecules suspended in buffer and milk solutions were used to test the detection capabilities of the device with excitation/emission wavelengths at 562 nm/584 nm and 650 nm/665 nm, respectively. We describe the different modules of the device and present a detailed experimental work performed to validate the device operation and extract performance parameters such as the limit of detection in terms of chromophore concentration, accuracy, sensitivity, and specificity. The obtained results demonstrate reliable detection of low chromophore concentrations (<100 pM), with repeatability and robustness confirmed under different conditions, making the MILI system an ideal candidate for rapid, cost-effective contamination detection device.


## 1 INTRODUCTION


The World Health Organization (WHO) has recognized food contamination as a global challenge in several reports (World Health Organization, 2015; Fukuda, 2015). Nearly 1 in 10 people worldwide become ill by consuming contaminated food, leading to 420,000 deaths annually (World Health Organization, 2022). For this reason, and as a legal and quality requirement for the dairy industry, controls must be performed in various stages of the value chain and in all batches of the final product. While pasteurization, a crucial step in milk processing, significantly reduces the risk of food-borne illnesses by eliminating most harmful pathogens, it does not address certain contaminants, such as chemical residues like Aflatoxin-M1 or residues from veterinary treatments, includ-


ing antibiotics (e.g., penicillin, enrofloxacin, sulfadioxine, streptomycin, trimethoprim, marbofloxacin). The presence of such substances in raw milk is regulated in most countries and even minute quantities will demand the discard of the milk (Olatoye et al., 2016), due to the severity of the impact on human health.

The dairy industry uses laboratory methods such as chromatography, immunoassays, and mass spectroscopy for the detection of Aflatoxin-M1 and antibiotics residues in milk (Gaudin, 2017; Vercelli et al., 2023; Getahun et al., 2023; Matabaro et al., 2017). Despite their precise and quantitative analysis of samples, these methods are time-consuming (up to 3 hours or even longer if outsourced), expensive and require specialised staff. Furthermore, they are usually performed after milk is loaded onto transport vehicles to dairy factories. Therefore, if a small portion of the loaded milk is contaminated, the contamination will spread to the whole load leading to wasted supply. Consequently, the financial losses to both the farmers (penalties based on regulation for deliver-

<sup>a</sup>  <https://orcid.org/0000-0001-5088-9029>

<sup>b</sup>  <https://orcid.org/0000-0001-5876-3922>

<sup>c</sup>  <https://orcid.org/0009-0005-3003-6519>

<sup>d</sup>  <https://orcid.org/0000-0002-4344-4416>

ing contaminated milk) and the receiving dairy factories (reduced milk quantities therefore production impacts) are vast. Rapid screening methods, such as lateral flow strips, can detect analytes within 10-40 minutes, but often generate a high rate of false positives and lack specificity for different types of antibiotics and in cases of positive results, a laboratory test confirmation is nevertheless needed, imposing additional costs and delays. These factors increase the need for the development of portable, highly integrated, and cost-effective devices in the field of food quality control. State-of-the-art concepts such as electrochemical (Singh et al., 2023; Reinholds et al., 2015), optical (Gastélum-Barrios et al., 2020; Yeh et al., 2017; Surkova et al., 2023; Souroullas et al., 2024), lab-on-a-chip (Buzzin et al., 2022; Manolis et al., 2024) techniques are being employed to achieve this.

In this work, we present a device aiming to solve these issues, through designing and developing a novel method to simultaneously detect in less than 10 minutes, a selected panel of common milk contaminants for analysis at the farm (before loading contaminated milk for transportation) and at the receiving dairy industry level. The MILI device is based on optical biosensors offering the analytical performance of laboratory-based methods, at a cost comparable to that of quick screening tests. The system is based on a sensitive mini-fluorometer setup that monitors the signal from fluorescence emitting biosensors that specifically bind on the selected analyte. The conceptual biosensor (not presented here) consists of derivatization and functionalization of a surface with antibodies specific to the selected contaminants. The recombinant or the natural antigen is labelled with a fluorophore and it is then mixed with the milk sample. The resulting solution is then added to the functionalized surface and the competition between labelled and unlabelled analytes inside the sample is evaluated by the emitted fluorescence intensity i.e. decrease with higher concentrations of the analyte in the sample (Pennacchio et al., 2016). Here, the capability of the device to detect contaminant concentrations dictated by EU regulations translated to merely dye-molecules or labelled antigens is demonstrated.

## 2 SYSTEM IMPLEMENTATION

This section describes: a) the system general architecture, b) the optical configuration, c) the overall integrated system, and d) the mobile application as the graphical user interface.

### 2.1 System Architecture

The general architecture of the MILI system presents the different units/modules of the system (Figure 1), as well as the user interaction that involves the manual import of the milk sample, and the control of the device and results visualisation via a mobile app. Focus is noted on the ‘Optical/Photonic Unit’ that consists of the excitation light source, the photodetector and the optical components, but also on the ‘Smart Cuvette Unit’ that consists of a functionalised cuvette, and temperature conditioning module to keep the sample at a stable temperature during measurements. Moreover, the main control unit is responsible for all system operations such as, controlling the excitation light source, acquiring the data from the detector, performing basic calculations and transmitting the analysis result to the mobile app. Finally, the power management module is responsible to provide the required power supply to all different parts of the system.

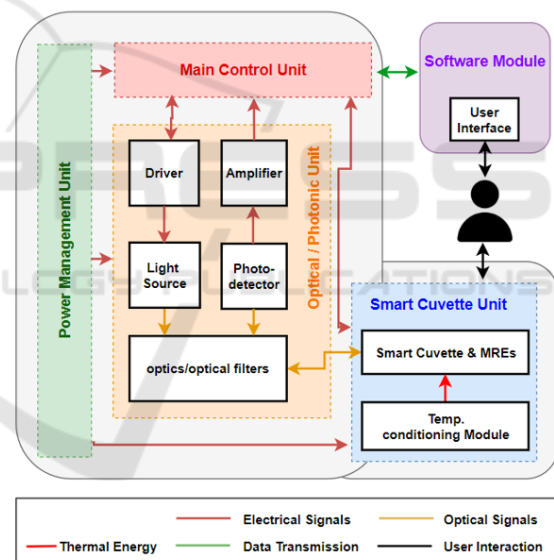


Figure 1: MILI System general architecture.

### 2.2 Optical Module

The optical configuration is based on a simple fluorometer configuration (Figure 2) where light emitted by the photo-excited sample can be measured. The optical components were chosen as to excite and detect fluorescence from specific dye molecules that are widely used to label antibodies specific to the analytes of interest. The MILI mini-fluorometer apparatus has been developed and evaluated in two different configurations which can be either used with the red CF@568 or the cyanine-based far-red CF@647 fluo-

rescent dyes. This was done to account from possible effects of the sample matrix when excited at different wavelengths i.e., emission from the sample itself which can shield the fluorophore signal. With this in mind, the system was designed to allow for a straightforward and easy switch between different configurations.

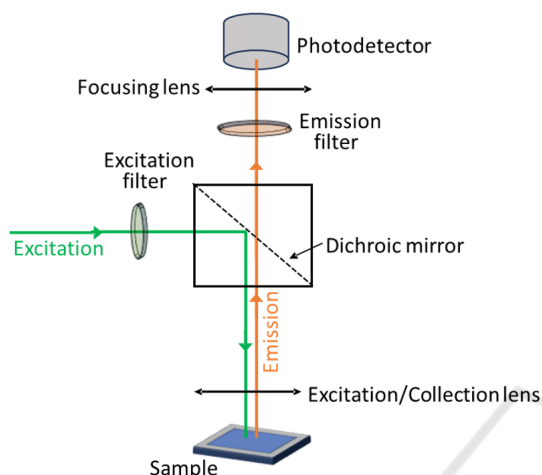


Figure 2: Fluorometer configuration. A light source excites a fluorescent sample which in turn emits at a different wavelength. The emitted light is then detected by a photodetector.

In order to achieve a satisfactory limit of detection (LOD) targeting 10 times less than the maximum residue limits of EU regulations (Regulation 37/2010, 2010), relatively high excitation powers had to be considered. This led to the use of a laser system as the excitation source instead of a cheaper light emitting diode (LED). Furthermore, due to the narrow bandwidth and optimised beam profile laser systems usually offer, a high signal-to-noise ratio (SNR) could be achieved which is essential for the detection of low fluorescence signals considered in these types of applications.

The experimental work conducted to validate the optical setup's capabilities and determine the lowest detectable dye concentration and thus the estimate the device's LOD included dye molecules suspended in Phosphate buffered saline (PBS) buffer to produce concentrations ranging from 10  $\mu\text{M}$  down to 0.1 pM. In all work presented in this paper, the samples were hosted in black-walled 96-well microplates suitable for fluorescence-based assays. It is noted that fluorescence emitted from samples of higher concentrations and down to 10 nM was easily observed and differentiated from background signal. For this reason, and for the fact that concentrations higher than 10 nM are irrelevant to the application in hand (outside of

the range set by EU regulations) results are presented only for lower concentrations.

### 2.2.1 Red Fluorescent Dye

The first configuration involved the case where the antibodies were to be labelled by a red fluorescent dye. The selected dye in this case was CF@568 with absorption and emission maxima at 562 nm and 584 nm, respectively. It is noted that this labelling reagent can be directly replaced by any of the following commercially available fluorophores: Alexa Fluor@568, ATTO 565, Rhodamine Red. Nevertheless, in this case the secondary excitation peak of CF@568 at 532 nm was chosen since monochromatic sources at this wavelength are more common and relatively cheaper. Thus, a diode pumped solid state (DPSS) laser source at 532 nm and maximum power of 40 mW was used as the excitation source also eliminating the need for a bandpass excitation filter due to its narrow linewidth  $\pm 1$  nm.

The light from the excitation source is incident on a single-edge dichroic mirror which reflects wavelengths below 550 nm. The reflected beam is then guided through an achromatic triplet lens system which focuses the beam on the sample area and also used to collect and colimate the emitted light from the sample. The emitted light then travels through the dichroic mirror and passes through an additional single-band emission filter centred at 580 nm thus further filtering wavelengths outside the chromophore emission range. Finally, the light is focused on to the PMT detector by an additional lens.

In this case the laser diode was modulated at 1 kHz allowing for a better visualisation of the difference between signal and background. The data collected during experiments showed that the LOD achievable by the device can be as low as 0.1 pM. Figure 3 shows the obtained fluorescence signal for the range of dye concentrations studied along with the modulation applied to the excitation source.

The obtained results highlight the capability of the MILI device to detect low concentrations of dye molecules (underestimate the LOD to 1 pM  $\sim$  0.0007 ppb for CF567 dye) which fall below the limits set by EU regulations regarding antibiotics and toxins. It can be safely assumed that this detection limit can be applied to the suggested biosensing assay where optimally one dye molecule binds to a single antigen. The effects of the milk matrix in real samples will be discussed later.

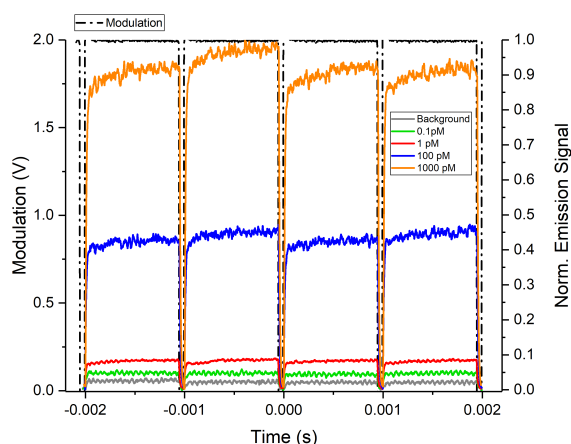


Figure 3: Modulation and normalised emission signal as recorded for CF568 diluted in PBS buffer solution for concentration range 0.1 – 1000 pM.

### 2.2.2 Cyanine-Based Far-Red Fluorescent Dye

The second configuration of the optical module considers the case of cyanine-based far-red chromophores also widely used in biosensing assays. Namely, results presented here were obtained by using the CF@647 with absorption and emission maxima at 650 nm and 665 nm, respectively. Similarly to the previous case, these dye molecules can be directly replaced by a set of other commercially available fluorophores such as Cy@5, Alexa Fluor@647, DyLight@649. The laser source used in this configuration has a nominal wavelength at 640 nm and maximum power of 35 mW.

The optics configuration is slightly modified from the previous dye case. The single-edge dichroic mirror now reflects wavelengths below 645 nm and an additional single-band bandpass optical filter centred at 642 nm is placed after the laser source to further reduce unwanted background light. The triplet lens system used for focusing the excitation beam and collecting the emitted fluorescence remains unchanged. The single-band emission filter is also switched to one that is centred at 670 nm.

The experiments with different dye concentration samples were repeated for this configuration. Figure 4 shows the signal recorded during these measurements. In this case the excitation source was not modulated but instead the concentration axis was plotted in logarithmic scale for a clearer representation. The plotted values are the result of the averaging of multiple measurements. It is obvious that fluorescence emission from the 0.01 pM sample can be differentiated from the background signal coming from the empty well or the PBS buffer sample. It should be noted that 2500 mV is the maximum signal the spe-

cific PMT can output, with values higher than this saturating the detector. For this reason, a combination of neutral density (ND) filters must be used in cases of higher concentrations to avoid PMT saturation even though this is not needed for this application purposes.

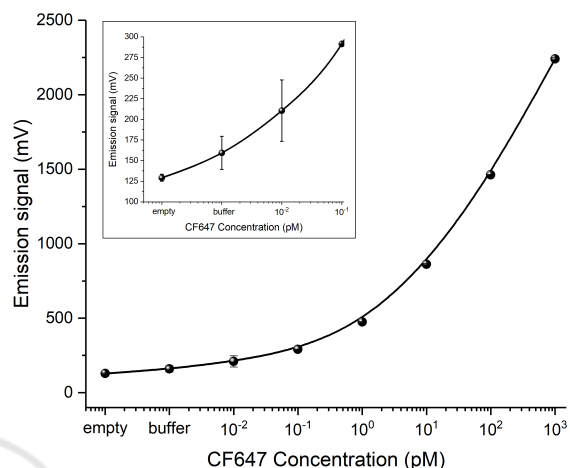


Figure 4: Fluorescence signal for different CF647 dye concentrations (0.01 – 1000 pM) as recorded by the MILI device. “Empty” denotes background signal from an empty well and “buffer” signal from merely PBS solution. The y-axis is in logarithmic scale.

## 2.3 System Integration

The device components are shown in Figure 5, consisting of the following main electronics parts: a) main control unit (MCU) with Bluetooth 5.0 connectivity, b) temperature controller with Peltier heat element and PT1000 temperature sensor for conditioning the sample’s temperature around 30 °C, c) device powering via four Li-Ion rechargeable batteries to extend the device operating hours (approximately 8 hours of continuous operation), d) a power bank module for charging the Li-Ion batteries via 5V USB, e) a DC/DC voltage converter (from 5V to  $\pm 5V$ ) for operating the PMT detector, and e) a DC/DC voltage converter (from 5V to 12V) for operating the laser.

Upon validating the optical configuration, the system was integrated to combine all modules (electronic, network, etc) and placed in an enclosure. The integrated MILI prototype device encapsulated in the custom 3D-printed black PLA material is presented in Figure 6, demonstrating a portable device for milk analysis capable of detection of contaminants in raw milk samples. It uses a single vial, detached from a black walled 96-well strip, as the sample-cuvette for performing analysis on 200  $\mu$ l of buffer-diluted raw milk samples. It has dimensions of 183 mm x 56 mm

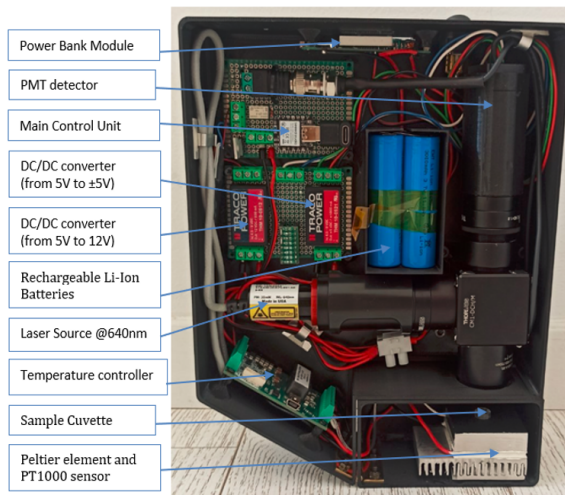


Figure 5: The integrated MILI prototype device in a custom 3D-printed housing.



Figure 6: The MILI prototype device as a portable device for milk analysis.

x 230 mm and weights 1.3 kg.

## 2.4 Mobile Application: Graphical User Interface

A mobile application was developed for the control and visualisation of the analysis procedure (Figure 7).

The application can automatically search and connect to a preconfigured (known MAC address) BLE device. Furthermore, the MCU is configured with a control-firmware to execute sequentially the following procedures for every analysis run: a) the MCU-Bluetooth (BLE) is advertising until a connection is established with the mobile application, b) the MCU waits for a BLE request via the 'Run Test' button on the mobile app graphical user interface (GUI), c) upon analysis request, a counter runs for a minute to allow the sample to reach a constant temperature at 30 °C, d) 10000 measurements are acquired from the PMT at a sampling rate of 1 Hz prior to switching on the laser; the average of these measurements represents the background or noise value, e) the laser switches ON and the system waits for 3 seconds to stabilize, f) 10000 measurements are acquired from the PMT at a sampling rate 1 Hz; the average of these measurements represents the milk-analysis signal, g) the MCU sends the result of the analysis in the form of 'positive' or 'negative' to the mobile app via the BLE connection and then the device is ready for the next analysis, where procedures c-g will be executed again.

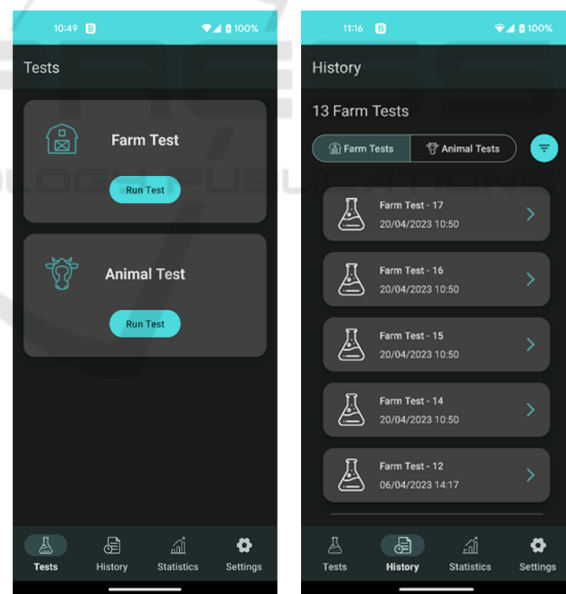


Figure 7: MILI mobile application used as the graphical user interface for control and visualisation of an analysis.

For the proper operation of the device, the user needs to follow the step-by-step instructions: a) Run the 'MILI app' and switch ON the MILI device. The device should be connected immediately with the mobile app and the green LED on the device left side will stop flashing periodically and will remain on; this confirms that the connectivity has been established

successfully, b) proceed to loading the sample-cuvette and press the ‘Run Test’ button on the application GUI, c) wait for approximately 2 minutes and press the ‘View Results’ button when it appears to view the results, d) access the menu on the bottom of the screen to check the historical and statistical results of the analysis (Figure 7).

### 3 PRELIMINARY TESTING

The MILI prototype has been tested for its functionality and general behaviour in different conditions such as: a) use of different types of sample-cuvettes: clear and black. Black cuvettes are more suitable for fluorescence measurements, while clear cuvettes are easily accessible, b) use with different types of milk samples: raw sheep, goat, cow as well as commercially available cow milk (milk fat content is considered as a variable parameter in the different milk types, which in some cases affects the results), c) use of different dilution of milk in PBS buffer i.e. 1% and 10% (this was based on previous experiments showing that 1% milk-buffer exhibits lower absorption of the excitation wavelength, while 10% aims at reduced dilution of the milk, resulting to higher analyte concentration in the sample), d) use of different fluorescent molecules i.e. CF647 molecules for calibration and characterisation purposes, and labelled penicillin-G (PenG) with CF647 simulating the analysis assay. The following experiments employ clear cuvettes with 1% and 10% milk-buffer samples, and three different milk types: goat, sheep, and commercially available milk, spiked with different CF647 dye concentrations. The results show higher background signal in the case of 1% milk-buffer ( $\sim 1000$  mV) (Figure 8a) compared to 10% ( $\sim 600$  mV) (Figure 8b). This is most likely due to increased reflection of the excitation light from the clear-cuvette walls, combined with the lower absorption from the milk matrix, resulting to a higher detectable background signal. The minimum detectable concentration is 100 pM especially in the case of 10% milk-buffer, where the background signal is lower. The worsening of the detectable limit compared to the results obtained prior integration is due to a combination of the effects originating from the milk matrix and use of compact electronics used to drive the integrated system in contrast with the transparent buffer solution and the more expensive laboratory equipment used during the evaluation experiments. Moreover, sheep milk has a higher fat content than goat milk which causes a lower fluorescence signal for the 100 pM dye-concentration, since fat further absorbs the excitation light, which in turn reduces photolumi-

nescence. Analogous behaviour is presented in the case of the commercial milk (Figure 8a), which contains less fat than both raw sheep and goat milk, therefore higher fluorescence signal is induced.

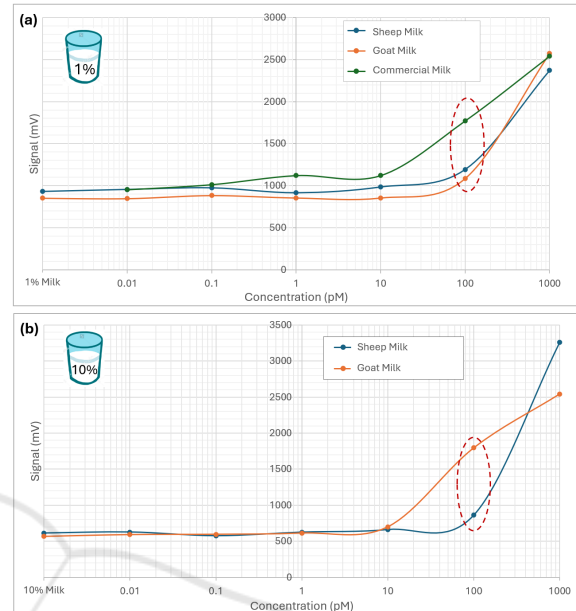


Figure 8: Tests with clear cuvettes and milk samples with (a) 1% and (b) 10% milk:buffer spiked with different CF647 dye concentrations.

Based on the above results, 10% milk-to-buffer ratio was used for the following experiments, where black cuvettes were tested. As expected, black cuvettes showed lower background signal, which in turn made the 10 pM dye concentration observable. On the other hand, 1 pM dye concentration can be barely considered detectable, since the voltage difference from the background signal almost falls within the signal noise level ( $\sim 30$  mV).

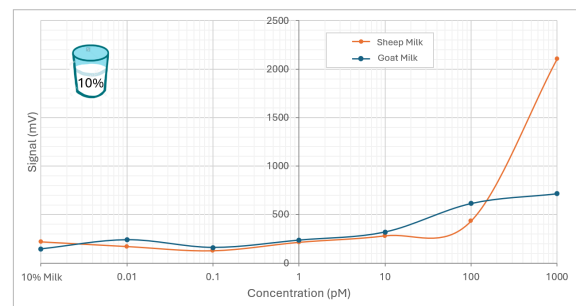


Figure 9: Tests with black cuvettes and 10% milk-buffer solutions at different dyes concentrations.

The next experiments used raw cow milk. Similarly, 10% milk-buffer samples have been tested (Figure 10a), while this time labelled PenG (PenG647)

was also used to spike the samples (Figure 10b). This was done to better simulate the real analysis assay where the analyte is PenG. Similar results with the other types of milk were obtained even with PenG647, with the 100 pM concentration being distinguishable from background in all cases.

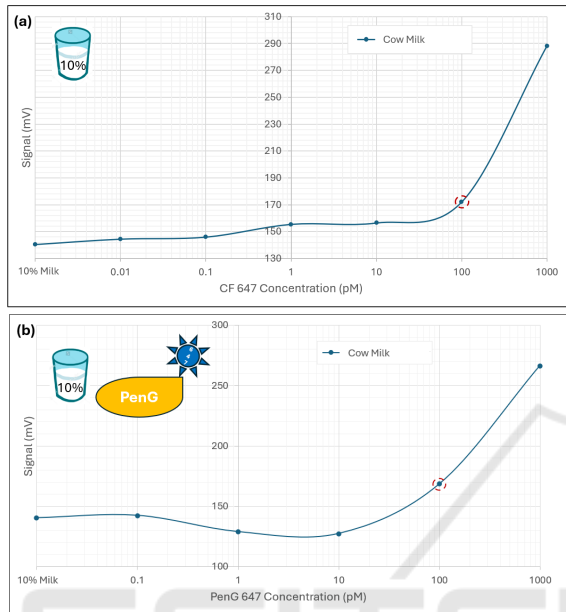


Figure 10: Tests with black cuvettes and raw cow milk with a) 10% milk-buffer at different CF647 concentrations, and b) spiked with PenG labelled with CF647.

#### 4 PERFORMANCE EVALUATION

For the next step of the validation process, more experiments defining the performance aspects of the prototype such as, the repeatability, reproducibility, accuracy, sensitivity, and specificity were conducted. Moreover, during these experiments the device was tested under different amplification settings on the photodetector, in order to change the dynamic range during measurements to the range of the interest, and thus detect dye concentrations up to 1000 pM.

For validating the repeatability and reproducibility, and hence the precision of measurement, tests were repeated multiple times on spiked milk samples (100, 200, 400, 1000 pM dye concentrations) collected from different batches and farms. It is noted that for each measurement performed the sample was removed from the device and placed again to check how user manual sample positioning affects the results. Furthermore, two different amplification settings on the photodetector were tested: 0.5V and 0.55V as the control voltage for the dedicated gains.

The results of these measurements are concluded in Table 1, that includes the calculated average value,  $A_v$ , standard deviation,  $\sigma$ , and coefficient of variation,  $CV$  for three different batches of milk at different dye-CF647 concentrations, as well as the overall average including all three types of milk. A relatively low ‘Coefficient of Variation’ has been acquired for all measurements, being below 20% which in general is considered as a ‘Very good’ and acceptable value. Furthermore, 2-3 times lower  $\sigma$  was observed (Table 1) when the photo-amplification was set at 0.5V opposed to the results with the higher amplification at 0.55V, which it was expected due to the increase of the photodetector noise with the increase of its amplification. Moreover, both amplification settings showed good linear behaviour (Figure 11), with  $R^2$  values to be higher than 0.9 which shows strong relation to a linear expression.

Table 1: Tests results for validating the repeatability and the reproducibility of the measurement. The names in the parenthesis next to the animal type is the location of the farm the milk was collected from.

Photoamplifier Gain (@0.55V)		Sheep (Dali)		Goat (Ioanna)		Goat (Paxna)		Overall Average	
Concentration (pM)	$A_v$ (mV) $\sigma$ CV (%)	$A_v$ (mV) $\sigma$ CV (%)	$A_v$ (mV) $\sigma$ CV (%)	$A_v$ (mV) $\sigma$ CV (%)	$A_v$ (mV) $\sigma$ CV (%)	$A_v$ (mV) $\sigma$ CV (%)	$A_v$ (mV) $\sigma$ CV (%)	$A_v$ (mV) $\sigma$ CV (%)	
10% milk-buffer	822 136 17	715 30 4	676 32 5	737 99 13					
100	843 61 7	787 50 6	774 5 1	801 52 6					
200	903 43 5	776 55 7	770 17 2	816 74 9					
400	945 28 3	914 42 5	886 69 8	915 51 6					
1000	1395 50 4	1238 151 12	1429 190 13	1354 156 12					

Photoamplifier Gain (@0.5V)		Sheep (Dali)		Goat (Ioanna)		Goat (Paxna)		Overall Average	
Concentration (pM)	$A_v$ (mV) $\sigma$ CV (%)	$A_v$ (mV) $\sigma$ CV (%)	$A_v$ (mV) $\sigma$ CV (%)	$A_v$ (mV) $\sigma$ CV (%)	$A_v$ (mV) $\sigma$ CV (%)	$A_v$ (mV) $\sigma$ CV (%)	$A_v$ (mV) $\sigma$ CV (%)	$A_v$ (mV) $\sigma$ CV (%)	
10% milk-buffer	264 18 7	272 40 15	261 31 12	266 28 11					
100	305 27 9	281 34 12	299 42 14	295 33 11					
200	378 26 7	351 2 1	359 29 8	363 24 7					
400	433 14 3	401 17 4	401 27 7	412 24 6					
1000	552 37 7	502 26 5	510 38 7	521 38 7					

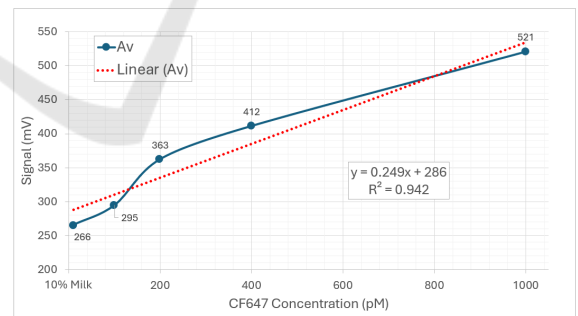


Figure 11: 10% raw cow milk-buffer spiked with CF647 at different concentrations, using detector amplification at 0.5V control voltage. Cuvette was repositioned before each measurement. The dashed line represents the linear fitting.

Subsequently, similar experiments with fresh-prepared samples were conducted, using photo-amplification at 0.5V control voltage. Again, each measurement was repeated several times for each concentration, but this time the sample was placed in the holder and the following measurements were executed one after the other without repositioning the

sample. This way, the experiment generated results on the reproducibility but also on the robustness of the measurement, correlated to the sample positioning executed by the user. Table 2 includes the previous (exchanging the cuvette) and the current (static cuvette) results for comparison. A general observation is that the standard deviation,  $\sigma$ , and consequently CV are only slightly lower in the case where the cuvette was static. Therefore, it can be considered that these results verify high measurement reproducibility and robustness related to sample positioning. In other words, the mechanical interface between the sample-holder and the optical apparatus, ensures reproducible results when it comes to the sample positioning practice applied by the user. Furthermore, the highly repeatable results (low  $\sigma$  and  $CV < 10\%$ ) in the case of the static-cuvette, show high measurement stability.

Table 2: Tests results for validating the reproducibility and robustness of the sample-positioning.

Static cuvette				Sheep (Dali)			Goat (Ioanna)			Goat (Paxna)			Overall Average		
Concentration (pM)	Av (mV)	$\sigma$	CV (%)	Av (mV)	$\sigma$	CV (%)	Av (mV)	$\sigma$	CV (%)	Av (mV)	$\sigma$	CV (%)	Av (mV)	$\sigma$	CV (%)
10% milk-buffer	361	15	4	322	10	3	350	5	1	320	19	6	320	19	6
100	375	16	4	335	8	2	390	4	1	356	25	7	356	25	7
200	390	9	2	391	4	1	405	5	1	379	9	2	379	9	2
400	429	9	2	441	9	2	444	20	4	426	12	3	426	12	3
1000	608	10	2	667	54	8	526	5	1	590	65	11	590	65	11

Exchangable cuvette				Sheep (Dali)			Goat (Ioanna)			Goat (Paxna)			Overall Average		
Concentration (pM)	Av (mV)	$\sigma$	CV (%)	Av (mV)	$\sigma$	CV (%)	Av (mV)	$\sigma$	CV (%)	Av (mV)	$\sigma$	CV (%)	Av (mV)	$\sigma$	CV (%)
10% milk-buffer	264	18	7	272	40	15	261	31	12	266	28	11	266	28	11
100	305	27	9	281	34	12	299	42	14	295	33	11	295	33	11
200	378	26	7	351	2	1	359	29	8	363	24	7	363	24	7
400	433	14	3	401	17	4	401	27	7	412	24	6	412	24	6
1000	552	37	7	502	26	5	510	38	7	521	38	7	521	38	7

Similarly, linear fitting was applied to the results as shown in Figure 12, to verify consistency with the previous results obtaining a higher  $R^2$  value equal to 0.998. Moreover, the flexibility of using the dynamic range for measuring higher concentration allowed for a quick test up to 10000 pM (10 nM), in order to check linearity at higher dye concentrations. The results are shown in Figure 12, where again the data are described by a linear relation with an  $R^2$  value close to unity.

Finally, the device performance in terms of accuracy, sensitivity and specificity was defined. Data from 120 tests (24 samples for each concentration – 0 pM, 100 pM, 200 pM, 400 pM, 1000 pM) in total were used to define true positives,  $TP$ , false negatives,  $FN$ , true negatives,  $TN$ , and false positives,  $FP$ . The same data was also used to calculate the above performance indicators based on the defined LOD (or cut-off value). Emphasis should be given in the definition of the LOD, considering that raw milk samples undergone 10% dilution, resulting to an analyte concentration of 10-times lower than in the initial raw sample. This means that the 100 pM, 200 pM and 400 pM referred LODs, correspond to 1 nM ( $\sim 1$  ppb), 2 nM ( $\sim 2$  ppb) and 4 nM ( $\sim 4$  ppb) concentrations in raw

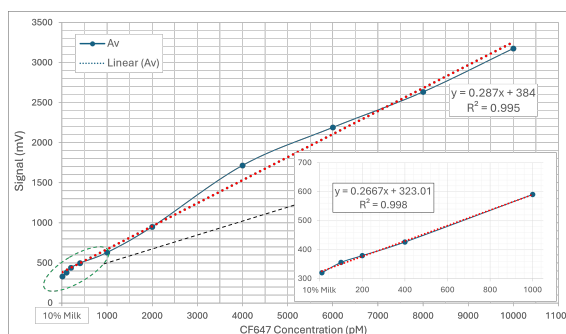


Figure 12: 10% raw cow milk-buffer spiked with CF647 at different concentrations. Cuvette position remained unchanged throughout data set. Inset: zoom in for dye concentrations below 1 nM. The red dashed line represents the linear fitting.

milk respectively. Satisfactory performance results ( $>80\%$ ) are presented in Table 3 for three different defined LODs. All three LODs present very good detection accuracy higher than 85%, while in each case sensitivity (related to  $FN$ ) competes specificity (related to  $FP$ ) and vice versa. Specifically, when requiring high sensitivity thus sacrificing specificity, LOD at 100 pM is preferable, while when requiring the opposite, LOD at 400 pM seems ideal with 100% specificity. In the case where a compromise is required, then an LOD at 200 pM gives sufficient performance values, between 83-90%. It is noted that the LOD values obtained by these validation experiments are comparable to other current works in the area of milk contaminant detection (Matabaro et al., 2017; Jalili et al., 2020).

Finally, in order to identify the integrity of the selected dye molecules for labelling the antibodies over time, a series of experiments was conducted to measure the emitted PL signal after storage. This work was performed as part of the optical configuration development to get an indication on the repeatability of the device in measuring identical samples at different points of time. Furthermore, the data collected here serve as a suggestion for the expiry period of the biosensors in terms of a consumable product in case of market exploitation. The degradation experiments consisted of different dye concentration samples prepared and assessed in different time intervals within a month to validate their integrity over time. The samples were prepared and stored at  $T = 5$  °C until the following measurement. Initially the measurements were performed after a few days apart and then performed weekly (Figure 13). Furthermore, new samples were prepared after 15 and 20 days from the initial preparation and the emitted signal was compared between old and new samples (not shown here). These experiments revealed a satisfactory consistency



Table 3: Performance indicators based on defined LOD.

**a) LOD=100pM & Cut-off value=320mV**

Total Positives	96
TP	86
FN	10
Total Negatives	24
TN	17
FP	7
Accuracy (%)	86
Specificity (%)	71
Sensitivity (%)	90

**b) LOD=200pM & Cut-off value=370mV**

Total Positives	72
TP	60
FN	12
Total Negatives	48
TN	43
FP	5
Accuracy (%)	86
Specificity (%)	90
Sensitivity (%)	83

**c) LOD=400pM & Cut-off value=410mV**

Total Positives	48
TP	39
FN	9
Total Negatives	72
TN	72
FP	0
Accuracy (%)	93
Specificity (%)	100
Sensitivity (%)	81

of fluorescence signal collected from the samples at different times. The small increase in signal that was observed between measurements comes from the fact that the buffer solution precipitated on the parafilm used to seal the samples during storage, thus slightly increasing the overall dye concentration. These results lead to the conclusions that (a) the device is capable of repeated measurements with high accuracy and (b) the choice of the labelling reagents is suitable for at least up to a month before mixing with real matrix samples.

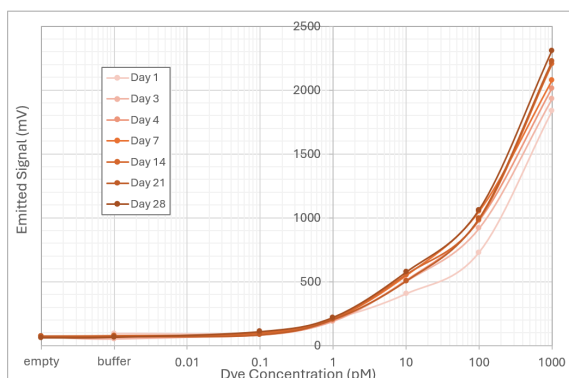


Figure 13: Degradation experiments for different concentrations of CF567 at different time intervals.

## 5 CONCLUSIONS

In conclusion, the MILI device different modules have been described in detail and validation experiments and their outcomes have been discussed. The optical module performed in a satisfactory fashion providing evidence for detection capabilities which allow for the recognition of contaminants (when bound to labelled antibodies) in concentrations that fall within the limits imposed by EU regulations. Furthermore, based on a comprehensive preliminary testing and performance evaluation of the MILI prototype, the results demonstrate that the device can reliably detect low concentrations of chromophores in various milk samples, with repeatability and robustness confirmed under different conditions. Overall, the device showed promising accuracy, and a LOD within the regulatory requirements for Penicillin-G detection in milk. These findings confirm that the MILI prototype is a potential tool for effective milk safety monitoring, meeting the targeted detection limits while maintaining high measurement consistency. The proposed technology aims to achieve a quality level of analysis equivalent to that provided by laboratories, without the need for trained personnel, providing results within 10 minutes and with costs that are significantly lower than those of the current market-available solutions. Overall, the MILI system seeks to reduce costs and improve contamination detection, offering a practical solution for early intervention and minimizing health risks and financial losses in the dairy supply chain.

## ACKNOWLEDGEMENTS

The work was supported by the Cyprus Research and Innovation Foundation grant EXCELLENCE/0421/0188 which is co-financed by the European Regional Development Fund and the Republic of Cyprus and by the European Union’s Horizon 2020 research and innovation programme “Code:Refarm” under grant agreement No 101000216.

## REFERENCES

Buzzin, A., Asquini, R., Caputo, D., and de Cesare, G. (2022). Evanescent waveguide lab-on-chip for optical biosensing in food quality control. *Photon. Res.*, 10(6):1453–1461.

Fukuda, K. (2015). Food safety in a globalized world. *Bull World Health Organ*, 93(4):212.

- Gastélum-Barrios, A., Soto-Zarazúa, G. M., Escamilla-García, A., Toledano-Ayala, M., Macías-Bobadilla, G., and Jauregui-Vazquez, D. (2020). Optical methods based on ultraviolet, visible, and near-infrared spectra to estimate fat and protein in raw milk: A review. *Sensors*, 20(12).
- Gaudin, V. (2017). Advances in biosensor development for the screening of antibiotic residues in food products of animal origin – a comprehensive review. *Biosensors and Bioelectronics*, 90:363–377.
- Getahun, M., Abebe, R. B., Sendekie, A. K., Woldeyohannis, A. E., and Kasahun, A. E. (2023). Evaluation of antibiotics residues in milk and meat using different analytical methods. *International Journal of Analytical Chemistry*, 2023(1):4380261.
- Jalili, R., Khataee, A., Rashidi, M.-R., and Razmjou, A. (2020). Detection of penicillin g residues in milk based on dual-emission carbon dots and molecularly imprinted polymers. *Food Chemistry*, 314:126172.
- Manolis, A., Eleftheriou, C., Elrabiaey, M. A., Tsekenis, G., D'Auria, S., Varriale, A., Capo, A., Staiano, M., Chmielak, B., Schall-Giesecke, A. L., Suckow, S., and Tsiokos, D. (2024). Ultra-fast detection of pathogens and protein biomarkers using a low-cost silicon plasmonic biosensing platform. *Sensors and Actuators Reports*, 8:100221.
- Matabaro, E., Ishimwe, N., Uwimbabazi, E., and Lee, B. H. (2017). Current immunoassay methods for the rapid detection of aflatoxin in milk and dairy products. *Comprehensive Reviews in Food Science and Food Safety*, 16(5):808–820.
- Olatoye, I. O., Daniel, O. F., and Ishola, S. A. (2016). Screening of antibiotics and chemical analysis of penicillin residue in fresh milk and traditional dairy products in Oyo state, Nigeria. *Vet World*, 9(9):948–954.
- Pennacchio, A., Varriale, A., Scala, A., Marzullo, V. M., Staiano, M., and D'Auria, S. (2016). A novel fluorescence polarization assay for determination of penicillin g in milk. *Food Chemistry*, 190:381–385.
- Regulation 37/2010 (2010). Commission Regulation (EU) No 37/2010 of 22 December 2009 on pharmacologically active substances and their classification regarding maximum residue limits in foodstuffs of animal origin. <https://eur-lex.europa.eu/legal-content/EN/TXT/?uri=celex%3A32010R0037>.
- Reinholds, I., Bartkevics, V., Silvis, I. C., van Ruth, S. M., and Esslinger, S. (2015). Analytical techniques combined with chemometrics for authentication and determination of contaminants in condiments: A review. *Journal of Food Composition and Analysis*, 44:56–72.
- Singh, B., Bhat, A., Dutta, L., Pati, K. R., Korpan, Y., and Dahiya, I. (2023). Electrochemical biosensors for the detection of antibiotics in milk: Recent trends and future perspectives. *Biosensors*, 13(9).
- Souroullas, K., Manoli, A., Itskos, G., Apostolou, T., and Papademas, P. (2024). Fluorescence of intrinsic milk chromophores as a novel verification method of uv-c treatment of milk. *Foods*, 13(18).
- Surkova, A., Bogomolov, A., Paderina, A., Khistiaeva, V., Boichenko, E., Grachova, E., and Kirsanov, D. (2023). Milk analysis using a new optical multisensor system based on lanthanide(III) complexes. *Engineering Proceedings*, 48(1).
- Vercelli, C., Amadori, M., Gambino, G., and Re, G. (2023). A review on the most frequently used methods to detect antibiotic residues in bovine raw milk. *International Dairy Journal*, 144:105695.
- World Health Organization (2015). WHO estimates of the global burden of foodborne diseases: foodborne diseases burden epidemiology reference group 2007–2015.
- World Health Organization (2022). Food safety. <https://www.who.int/news-room/fact-sheets/detail/food-safety>.
- Yeh, P., Yeh, N., Lee, C.-H., and Ding, T.-J. (2017). Applications of LEDs in optical sensors and chemical sensing device for detection of biochemicals, heavy metals, and environmental nutrients. *Renewable and Sustainable Energy Reviews*, 75:461–468.